

BDH2 Inhibits Lung Adenocarcinoma Metastasis by Promoting Ferroptosis

Qiao Yang¹ · Lin Tian² · Xiaodong Chen¹ · Xiong Mei¹✉ · Yongli Nie¹ · Jun Chen³

Abstract

To investigate the role of 3-hydroxybutyrate dehydrogenase 2 (BDH2) in regulating ferroptosis and its impact on the metastasis of lung adenocarcinoma (LUAD). Expression levels of BDH2 were modulated in LUAD cell lines (A549, PC9) using pcDNA-BDH2 plasmid transfection. Cell motility was assessed by Transwell assays, while ferroptosis-associated markers, including Fe²⁺, malondialdehyde (MDA), lipid reactive oxygen species (ROS), ACSL4, and GPX4, were evaluated by biochemical assays, flow cytometry, and Western blotting. The involvement of the Nrf2/HO-1 signaling axis was analyzed by Western blotting and RT-qPCR. Furthermore, a xenograft mouse model was established to confirm the effect of BDH2 on tumor progression and metastasis *in vivo*. Overexpression of BDH2 significantly inhibited LUAD cell migration and invasion. BDH2 upregulation enhanced ferroptosis, effects that were reversed by the ferroptosis inhibitor Fer-1. Mechanistically, BDH2 suppressed the activation of the Nrf2/HO-1 pathway, thereby enhancing sensitivity to ferroptosis. *In vivo*, BDH2 overexpression markedly reduced tumor growth and metastasis in nude mice, while inhibition of ferroptosis attenuated these effects. BDH2 suppresses metastasis in LAUD by promoting ferroptosis via suppression of the Nrf2/HO-1 pathway, highlighting BDH2 as a potential therapeutic target for LUAD.

Keywords

BDH2 · lung adenocarcinoma · ferroptosis · metastasis · Nrf2/HO-1 signaling · SLC7A11

Received: 14 October 2025 / Accepted: 6 February 2026 /

© L. Hirszfeld Institute of Immunology and Experimental Therapy, Wrocław, Poland 2025

Abbreviations

ACSL4, acyl-CoA synthetase long-chain family member 4; ALK, anaplastic lymphoma kinase; EGFR, epidermal growth factor receptor; GPX4, glutathione peroxidase 4; KRAS, Kirsten rat sarcoma viral oncogene homolog; Nrf2/HO-1, nuclear factor erythroid 2-related factor 2 / heme oxygenase-1; pcDNA-BDH2, BDH2 overexpression plasmid based on the pcDNA vector; RIPA, radioimmunoprecipitation assay; RNA, ribonucleic acid; RT-qPCR, reverse transcription-quantitative polymerase chain reaction; SLC7A11, solute carrier family 7 member 11.

1. Introduction

Lung cancer remains the leading cause of cancer-related mortality worldwide, accounting for nearly one-fifth of all cancer deaths annually (Lovly 2022). Among its histological subtypes, lung adenocarcinoma (LUAD) is the most prevalent form (Wei et al. 2023). LUAD is characterized by an aggressive biological behavior, including rapid progression, high

metastatic potential, and frequent therapeutic resistance, all of which contribute to its poor prognosis (Denisenko et al. 2018; Wei et al. 2023). Despite advances in surgical techniques, radiotherapy, chemotherapy, immunotherapy, and molecularly targeted therapies, the overall 5-year survival rate for patients with LUAD remains below 20% (Chen et al. 2024). This pressing clinical challenge underscores the urgent need to identify novel targets and therapeutic strategies to improve patient outcomes.

Ferroptosis, a recently recognized form of regulated cell death, is distinct from apoptosis, necrosis, and autophagy (Lei et al. 2022). It is characterized by iron-dependent accumulation of lipid peroxides, leading to catastrophic oxidative damage within the cell (Feng et al. 2023). Growing evidence suggests that ferroptosis is intimately associated with cancer biology, acting as either a tumor suppressive or tumor-promoting mechanism depending on the cellular and microenvironmental context (Cao and Dixon 2016). In LUAD, ferroptosis has emerged as a critical regulator of tumor initiation, progression, and metastasis (Zuo et al. 2025). Several studies have revealed that modulating ferroptosis-related pathways, such as SLC7A11, GPX4, and the Nrf2/HO-1 axis, significantly affects tumor growth and therapeutic response (Xu et al. 2025). These findings highlight ferroptosis not only as a fundamental biological process but also as a promising therapeutic target in LUAD.

3-Hydroxybutyrate dehydrogenase 2 (BDH2), also known as DHRS6, is a cytosolic enzyme belonging to the

¹Department of Oncology, Sinopharm Han Jiang Hospital, Shiyan City, Hubei Province, 442700, China

²Department of Medicine, Wuhan Wuchang Hospital, Wuhan, Hubei Province, 430063, China

³Experimental Center, Sinopharm Dongfeng General Hospital, Hubei University of Medicine, Shiyan City, Hubei Province, 442008, China

✉ nieyongli_dr@163.com

short-chain dehydrogenase/reductase family (Liu et al. 2020). Encoded on human chromosome 4q, BDH2 produces a 245-amino acid protein with dual biological functions. It participates in ketone body utilization by converting 2-hydroxybutyrate, and it catalyzes the biosynthesis of 2,5-dihydroxybenzoic acid (2,5-DHBA), a mammalian siderophore essential for iron binding and homeostasis (Li et al. (2024). Beyond its metabolic roles, BDH2 has been implicated in cancer biology. For example, it has been identified as a poor prognostic marker in acute myeloid leukemia, possibly due to its anti-apoptotic function, and its expression is regulated by long non-coding RNAs in esophageal cancer (Wenqiao et al. 2016). However, whether BDH2 influences LUAD metastasis, particularly through the regulation of ferroptosis, has not yet been elucidated.

In this study, we investigated the role of BDH2 in regulating ferroptosis and its impact on LUAD metastasis. By integrating both *in vitro* and *in vivo* models, we aim to determine whether BDH2 suppresses tumor invasion and metastasis through the induction of ferroptosis and modulation of the Nrf2/HO-1 axis.

2. Materials and Methods

2.1 Cell culture and transfection

According to the Cellosaurus database, A549 and PC9 cells harbor unfavorable prognostic mutations and exhibit limited sensitivity to currently available targeted therapies, supporting their use as suitable models for exploring alternative therapeutic strategies such as ferroptosis. Human LUAD cell lines A549 and PC9 were obtained from the American Type Culture Collection (ATCC). Cells were cultured in RPMI-1640 medium (11875093, Gibco, Grand Island, NY, USA) supplemented with 10% fetal bovine serum (FBS) (10099141C, Gibco, USA) in a humidified incubator with 5% CO₂. For gene overexpression, the BDH2 plasmid was purchased from Addgene (Watertown, MA, USA), and transient transfection was performed using Lipofectamine 3000 (L3000015, Invitrogen, USA). Both A549 and PC9 cells were transfected either with an empty control plasmid (pcDNA) or a BDH2 overexpression plasmid (pcDNA-BDH2). Each cell line was subsequently divided into control and experimental groups for downstream analyses. Lentiviral particles used for stable transduction were provided by HGY Biotechnology (Wuhan, China).

2.2 Reagents and treatments

Ferrostatin-1 (SML0583, Sigma-Aldrich, USA) and Erastin (SML2289, Sigma-Aldrich, USA) were used as ferroptosis inhibitors and inducers, respectively. Most general-purpose reagents, including RIPA buffer (P0013B, Beyotime, Shanghai, China), BCA protein assay kit (P0012, Beyotime,

China), enhanced chemiluminescence (ECL) detection kit (P0018FS, Beyotime, China), and JC-1 kit (C2006, Beyotime, China), were purchased from Beyotime. The Fe²⁺ assay kit (E1042, Beyotime, China), malondialdehyde (MDA) assay kit (S0131S, Beyotime, China), and reactive oxygen species (ROS) detection kit (S0033M, Beyotime, China) were used for biochemical analyses.

2.3 Western blotting

Cells were lysed in RIPA buffer supplemented with protease and phosphatase inhibitors. Protein samples (20–30 µg) were separated by sodium dodecyl sulfate–polyacrylamide gel electrophoresis (SDS-PAGE) and transferred to polyvinylidene fluoride (PVDF) membranes. After blocking with 5% non-fat milk in Tris-buffered saline with Tween 20 (TBST), membranes were incubated with primary antibodies overnight at 4°C. The following antibodies were used: anti-BDH2 (ab134938, Abcam, 1:1000); anti-ACSL4 (ab155282, Abcam, 1:1000); anti-GPX4 (ab125066, Abcam, 1:2000); anti-Nrf2 (ab62352, Abcam, 1:1000); anti-HO-1 (ab13243, Abcam, 1:1000); anti-GAPDH (ab8245, Abcam, 1:5000). After washing, membranes were incubated with HRP-conjugated secondary antibodies (ab205718, Abcam, 1:5000) for 1 h at room temperature. Protein bands were visualized using an ECL detection kit.

2.4 Cell motility assays

Cell migration and invasion were evaluated using Transwell chambers (3422, Corning, Corning, NY, USA) with or without Matrigel coating (354234, Corning, USA). Cells were seeded into the upper chambers in serum-free medium, while the lower chambers contained medium with 10% FBS. After 24 h of incubation, migrated or invaded cells were fixed with 4% paraformaldehyde (P0099, Beyotime, China) and stained with crystal violet (C0121, Beyotime, China). Images were acquired using an inverted microscope (Olympus, Tokyo, Japan).

2.5 Flow cytometry analysis

Intracellular ROS levels were measured with a DCFH-DA probe (S0033M, Beyotime, China). Briefly, cells were incubated with 10 µM probe for 30 min at 37°C, washed twice with phosphate-buffered saline (PBS) to remove excess stain, and immediately analyzed using a flow cytometer (BD Biosciences, USA). Fluorescence intensity was quantified to assess intracellular ROS levels.

2.6 Animal experiments

All animal experiments were performed in accordance with the guidelines approved by the Medical Ethics Committee

of Sinopharm Han Jiang Hospital. Notably, 6-week-old male BALB/c nude mice were purchased from Vital River Laboratory Animal Technology Co., Ltd. (Beijing, China). A549 cells transfected with pcDNA, pcDNA-BDH2, or pcDNA-BDH2 combined with Fer-1 treatment were subcutaneously injected into the flanks of nude mice ($n = 6$ per group). Tumor volume was monitored every 7 days using caliper measurements, and tumor weight was recorded at the endpoint. Tissues were excised, fixed in 4% paraformaldehyde, embedded in paraffin, sectioned, and subjected to H&E staining (C0105, Beyotime, China) for histological analysis.

2.7 Statistical analysis

All experiments were performed in triplicate, and data are presented as the mean \pm standard deviation (SD). Statistical

comparisons were conducted using one-way ANOVA. A p -value of < 0.05 was considered statistically significant.

3. Results

3.1 BDH2 suppresses migration, invasion, and epithelial-mesenchymal transition in LUAD cells

To determine whether BDH2 affects the motility of LUAD cells, we examined its expression and functional effects in A549 and PC9 cells. Western blot analysis confirmed that BDH2 protein levels were efficiently upregulated following transfection with pcDNA-BDH2 (Figure 1a). Transwell assays further demonstrated that BDH2 overexpression significantly decreased the number of migrating and invading cells in both LUAD cell lines (Figure 1b). Collectively, these findings indicate that BDH2 inhibits the migratory and invasive capabilities of LUAD cells.

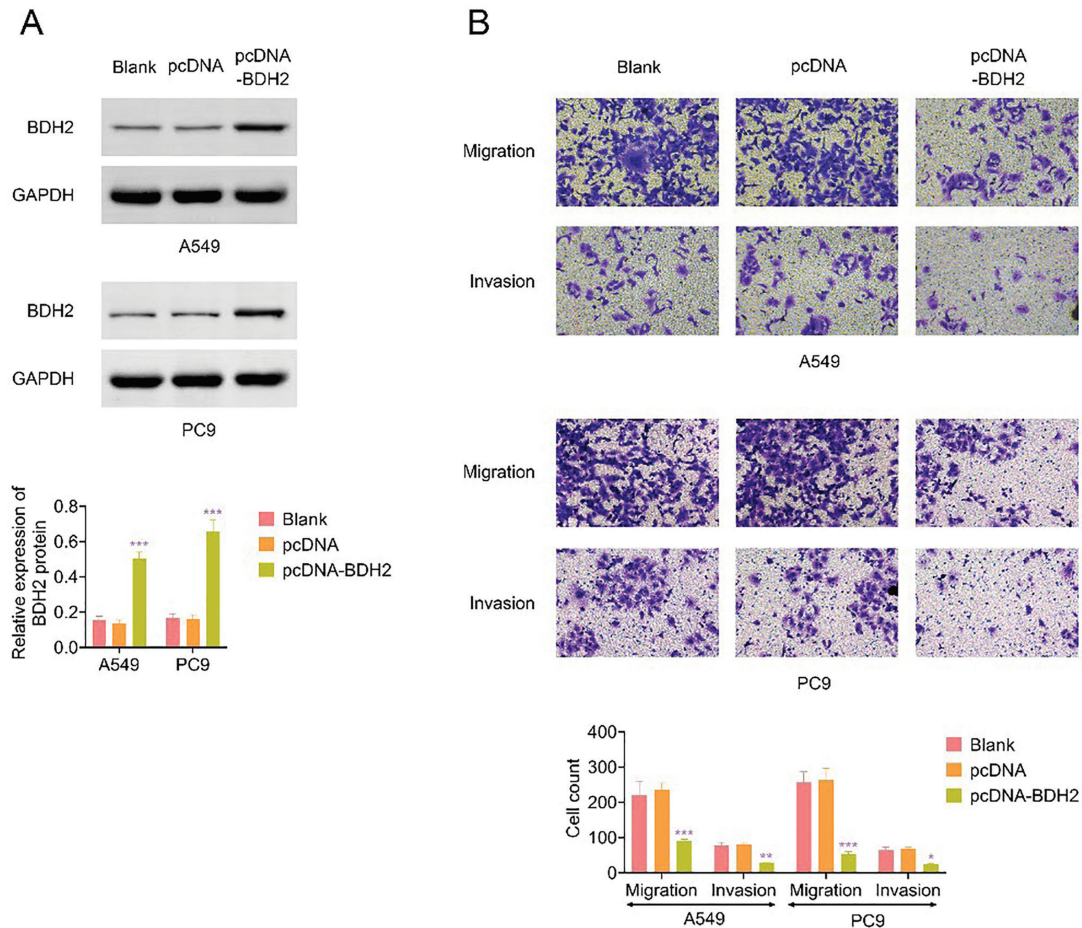


Fig 1. BDH2 inhibits migration, invasion, and EMT of LUAD cells. **(A)** Western blot analysis of BDH2 protein expression in A549 and PC9 cells following transfection with empty vector (pcDNA) or BDH2-overexpressing plasmid (pcDNA-BDH2). GAPDH was used as a loading control. Quantification of BDH2 protein levels is shown below. **(B)** Representative images of Transwell migration and invasion assays performed in A549 and PC9 cells after transfection with pcDNA or pcDNA-BDH2. Quantitative analysis of migrated and invaded cells is presented in the bar graphs. Data are presented as mean \pm SD. *** $p < 0.001$. EMT, epithelial–mesenchymal transition; LUAD, lung adenocarcinoma; SD, standard deviation.

3.2 BDH2 promotes ferroptosis to inhibit LUAD cell migration and invasion

We next investigated whether ferroptosis contributes to the inhibitory effects of BDH2 on metastasis in LUAD cells. Measurement of intracellular Fe^{2+} levels revealed elevated iron concentrations following BDH2 overexpression, which were attenuated by the ferroptosis inhibitor Ferrostatin-1 (Fer-1) but further enhanced by the ferroptosis inducer Erastin (Figure 2a). A similar trend was observed for lipid peroxidation, as shown by MDA quantification, which confirmed the induction of a ferroptotic phenotype (Figure 2b). In parallel, Western blot analyses revealed upregulation of ACSL4 and downregulation of GPX4 in pcDNA-BDH2-transfected cells, with Fer-1 reversing and Erastin amplifying these effects (Figure 2c). Together, these data suggest that BDH2 enhances ferroptosis to suppress LUAD cell migration and invasion.

3.3 BDH2 modulates the Nrf2/HO-1 axis

To further explore the molecular mechanism underlying BDH2-induced ferroptosis, we evaluated the Nrf2/HO-1 signaling cascade. Overexpression of BDH2 led to a reduction in Nrf2 and HO-1 protein levels in both A549 and PC9 cells (Figure 3). Quantitative analysis corroborated the suppression of this antioxidant pathway. These findings suggest that BDH2 may enhance ferroptotic sensitivity by negatively regulating the Nrf2/HO-1 axis.

3.4 BDH2 inhibits LUAD tumor growth and metastasis *in vivo* through ferroptosis

We next validated the tumor-suppressive role of BDH2 *in vivo* using a xenograft mouse model. Nude mice injected with A549 cells transfected with pcDNA-BDH2 developed

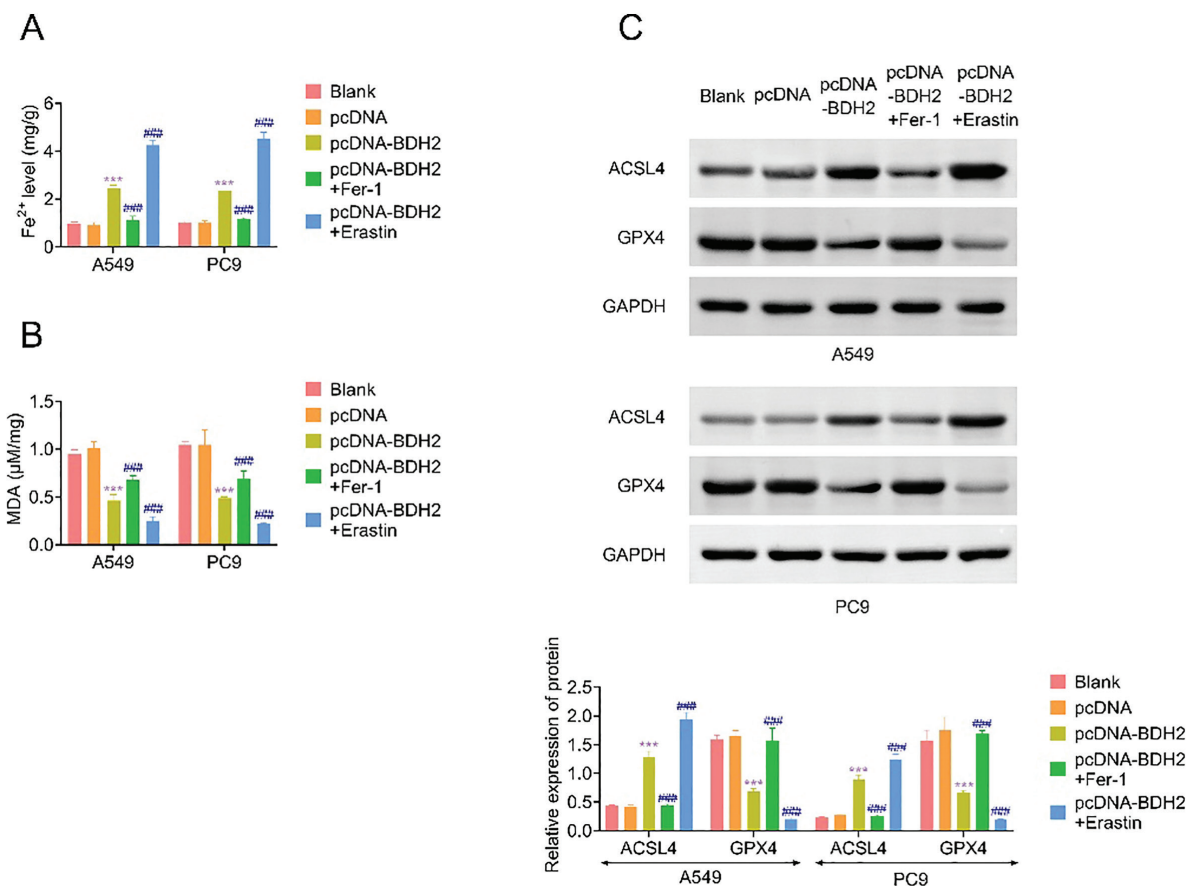


Fig 2. BDH2 suppresses migration and invasion of LUAD cells by promoting ferroptosis. (A) Measurement of intracellular Fe^{2+} levels in A549 and PC9 cells under different conditions: Blank, pcDNA, pcDNA-BDH2, pcDNA-BDH2 + ferroptosis inhibitor (Fer-1), and pcDNA-BDH2 + ferroptosis inducer (Erastin). (B) Measurement of MDA levels in A549 and PC9 cells under the same experimental conditions. (C) Western blot analysis of ACSL4 and GPX4 protein expression in A549 and PC9 cells across different groups. GAPDH was used as a loading control. Quantification of protein expression levels is shown below. Data are presented as mean \pm SD. *** $p < 0.001$ vs control; #### $p < 0.001$ vs pcDNA-BDH2 group. BDH2, 3-Hydroxybutyrate dehydrogenase 2; LUAD, lung adenocarcinoma; MDA, malondialdehyde; SD, standard deviation.

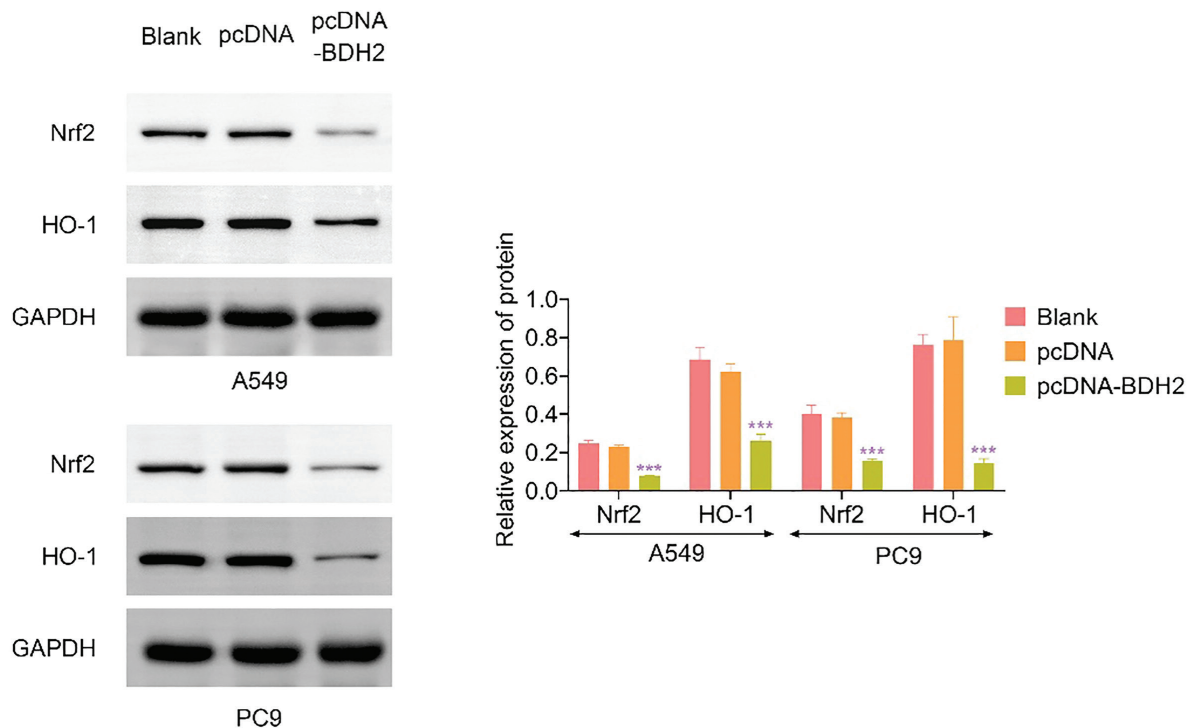


Fig 3. BDH2 regulates the Nrf2/HO-1 axis in LUAD cells. Western blot analysis of Nrf2 and HO-1 protein expression in A549 and PC9 cells after transfection with pcDNA or BDH2-overexpressing plasmid (pcDNA-BDH2). GAPDH was used as a loading control. Quantitative analysis of protein expression levels is shown in the bar graphs. Data are presented as mean \pm SD. *** p < 0.001 vs control. LUAD, lung adenocarcinoma; SD, standard deviation.

significantly smaller tumors compared with the control group, while co-treatment with the ferroptosis inhibitor Fer-1 partially restored tumor volume and weight (Figure 4a). Additionally, histological analysis revealed fewer metastatic nodules in the BDH2-overexpression group, whereas Fer-1 attenuated this suppressive effect (Figure 4b). Taken together, these findings indicate that BDH2 suppresses tumor growth and metastasis *in vivo* by promoting ferroptosis.

4. Discussion

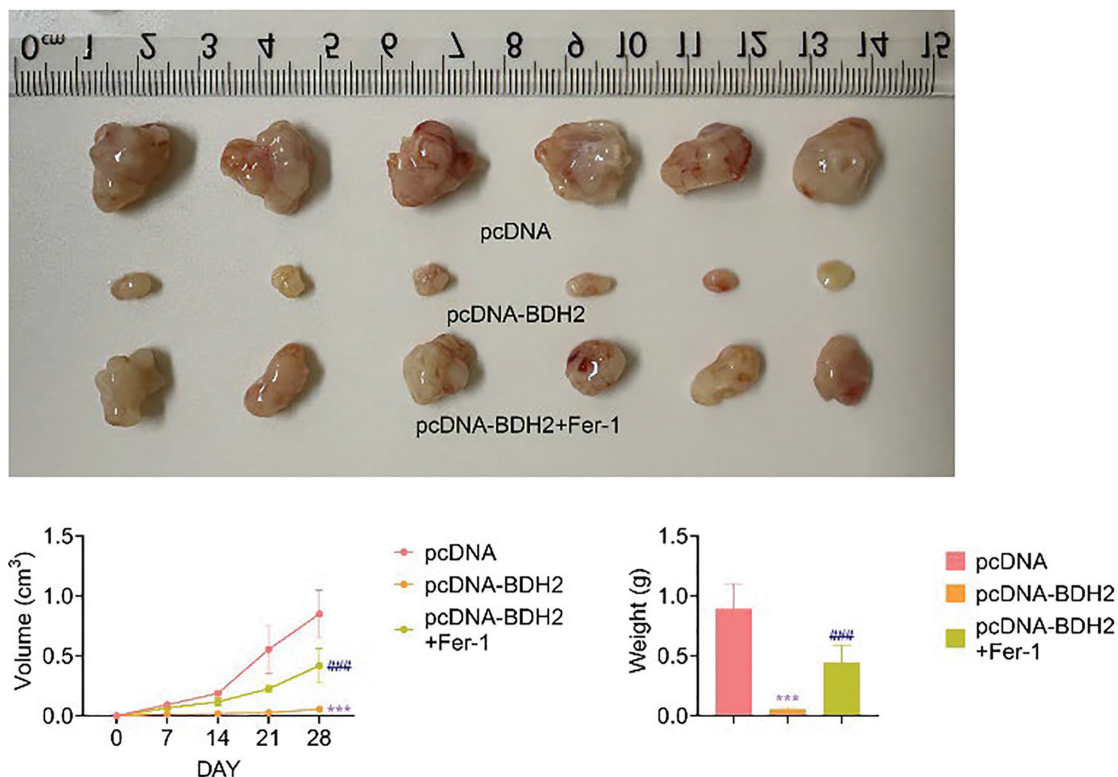
LUAD is the most common histological subtype of lung cancer (Wei et al. 2023). Despite recent advances in molecular-targeted therapies and immunotherapies, the clinical outcome for LUAD remains poor, with a 5-year survival rate of less than 20% (Denisenko et al. 2018). This is largely attributable to the aggressive nature of LUAD, high metastatic potential, and the frequent emergence of drug resistance. Current targeted therapies mainly focus on oncogenic drivers, such as EGFR, ALK, and KRAS; however, many patients lack actionable mutations or eventually develop resistance, thereby necessitating the identification of novel therapeutic strategies (Wu et al. 2021). In this context, our study identifies BDH2 as a potential suppressor of LUAD metastasis through the modulation of

ferroptosis, introducing an alternative therapeutic axis that may complement existing approaches.

BDH2 is a short-chain dehydrogenase/reductase enzyme that plays important roles in ketone body metabolism and iron homeostasis (Scindia et al. 2022). In recent years, BDH2 has been implicated in various pathological conditions (Tandon et al. 2023). For instance, it has been identified as a poor prognostic marker in acute myeloid leukemia due to its anti-apoptotic activity, while in esophageal squamous cell carcinoma, BDH2 expression is regulated by long non-coding RNAs that influence cell proliferation and apoptosis (Seah et al. 2025). Our findings extend these observations to LUAD by demonstrating that BDH2 overexpression markedly suppresses migration and invasion in LUAD cells. This suggests that BDH2 may function as a tumor suppressor in LUAD, in contrast to its context-dependent oncogenic role in other malignancies.

To further delineate the role of BDH2 in LUAD, we employed *in vitro* and *in vivo* models to manipulate its expression. We observed that BDH2 overexpression not only inhibited cell proliferation but also enhanced ferroptotic susceptibility, thereby attenuating metastatic behavior. Specifically, BDH2 significantly elevated intracellular Fe^{2+} levels, increased lipid peroxidation, and induced changes in ferroptosis-associated proteins, such as upregulation of

A



B

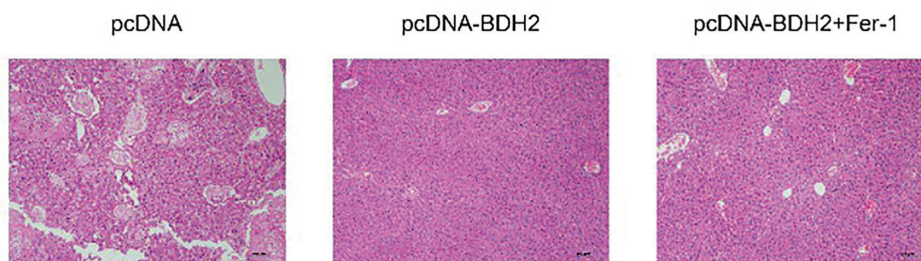


Fig 4. BDH2 inhibits tumor metastasis in vivo by promoting ferroptosis in LUAD cells. **(A)** Representative images of xenograft tumors derived from A549 cells transfected with pcDNA, pcDNA-BDH2, or pcDNA-BDH2 combined with ferroptosis inhibitor (Fer-1). Tumor growth curves and tumor weights are shown in the corresponding graphs. **(B)** Representative hematoxylin and eosin (H&E) staining of tissue sections from nude mice in different groups, used to evaluate metastatic lesions. Data are presented as mean \pm SD. *** p < 0.001 vs control; ### p < 0.001 vs pcDNA-BDH2 group. LUAD, lung adenocarcinoma; SD, standard deviation.

ACSL4 and downregulation of GPX4. These results underscore that BDH2 influences both the proliferative and migratory capacity of LUAD cells by promoting ferroptotic cell death. Collectively, our cellular models provide strong evidence that BDH2-driven ferroptosis serves as a key mechanism restraining LUAD progression.

Ferroptosis is an iron-dependent form of regulated cell death characterized by the accumulation of lipid peroxides and ROS (Yi et al. 2024). Unlike apoptosis or necrosis, ferroptosis is driven by distinct metabolic and redox pathways (Wei et al. 2024). Key regulators include the SLC7A11, GPX4,

and enzymes associated with lipid remodeling, such as ACSL4 (Cui et al. 2021). In this study, we found that BDH2 overexpression led to enhanced ferroptotic phenotypes, evidenced by higher lipid ROS and MDA levels, as well as altered expression of GPX4 and ACSL4. These findings are consistent with previous reports demonstrating that ferroptosis not only restricts tumor cell viability but also enhances sensitivity to anticancer therapies, such as cisplatin-based chemotherapy (Rizzollo et al. 2025). Thus, BDH2 may function as a molecular amplifier of ferroptosis, thereby suppressing LUAD malignancy.

An additional mechanistic layer uncovered in our work is the regulation of the Nrf2/HO-1 signaling pathway by BDH2. Nrf2 is a master transcriptional regulator of antioxidant defense and cellular redox homeostasis, while HO-1 serves as a downstream effector with well-established cytoprotective functions (Wu et al. 2022). Aberrant activation of this pathway has been associated with ferroptosis resistance and tumor progression in LUAD (Zhu et al. 2025). Our data demonstrate that BDH2 overexpression suppresses the Nrf2/HO-1 axis, thereby reducing the antioxidant capacity of LUAD cells and facilitating ferroptosis induction. These findings suggest that BDH2 may increase ferroptotic vulnerability by disrupting redox homeostasis, further supporting its tumor-suppressive function. Notably, several clinically used drugs, including sorafenib and cisplatin, have been shown to induce ferroptosis as a secondary mechanism, thereby contributing to their antitumor efficacy across multiple cancer types. Moreover, emerging clinical trials targeting ferroptosis-related pathways, such as system Xc⁻ inhibition or GPX4-associated redox regulation, further support the translational relevance of ferroptosis-based strategies. Evidence from hepatocellular carcinoma, renal cell carcinoma, and non-small cell lung cancer suggests that ferroptosis induction can effectively suppress tumor growth and overcome therapeutic resistance. Future research should therefore focus on developing pharmacological approaches to modulate the BDH2–ferroptosis axis and assessing their therapeutic efficacy in preclinical and clinical settings. Importantly, combining ferroptosis-inducing agents with conventional chemotherapy, targeted therapy, or immunotherapy may represent a promising polytherapy strategy, potentially enhancing antitumor efficacy relative to monotherapy.

Several limitations of this study should be acknowledged. First, our findings are based on established LUAD cell lines and xenograft models, which may not fully exhibit the biological complexity of human LUAD. Validation in patient-derived xenografts or organoid models would provide stronger translational relevance. Second, although we identified ferroptosis and Nrf2/HO-1 signaling as key mediators, other pathways influenced by BDH2 remain unexplored. In this study, A549 cells were selected for *in vivo* experiments due to their consistent tumorigenic capacity and reproducibility in nude mouse xenograft models. While this choice ensured experimental robustness, future studies incorporating additional LUAD cell lines or patient-derived xenografts will be important to further validate the generalizability of our findings. Future work should investigate the broader regulatory network of BDH2, including potential crosstalk with metabolic and immune-related pathways. Moreover, clinical data linking BDH2 expression with patient prognosis in LUAD are currently lacking. Large-scale clinical cohorts and retrospective analyses will be required to evaluate its potential utility as a prognostic biomarker. Finally, a key methodological limitation is that BDH2 overexpression

in this study was achieved via plasmid-based gene delivery, a technique not yet feasible for direct clinical application in humans. Therefore, our findings should be interpreted as proof-of-concept, highlighting the therapeutic potential of targeting the BDH2–ferroptosis axis, rather than proposing an immediately translatable clinical intervention.

Therefore, BDH2 acts as a suppressor of LUAD metastasis by promoting ferroptosis through inhibition of the Nrf2/HO-1 signaling pathway. These findings provide novel mechanistic insights into the regulation of ferroptosis in LUAD and highlight BDH2 as a promising therapeutic target for limiting metastasis and improving patient outcomes.

Acknowledgements

Not applicable.

Funding

This work was supported by the Guiding Scientific Research Project of Shiyuan Science and Technology Bureau in 2024 (Grant No. 2024-163).

Competing Interests

The authors state that there are no conflicts of interest to disclose.

Ethics Approval

Ethical approval was obtained from the Medical Ethics Committee of Sinopharm Han Jiang Hospital (Approval no. 2024-01)

Data Availability

The authors declare that all data supporting the findings of this study are available within the paper, and any raw data can be obtained from the corresponding author upon request.

Contribution of Authors

Qiao Yang and Lin Tian designed the study and carried it out. Qiao Yang, Lin Tian, Xiaodong Chen, Xiong Mei, and Yongli Nie supervised the data collection. Qiao Yang, Lin Tian, Xiaodong Chen, Xiong Mei, and Yongli Nie analyzed the data. Qiao Yang, Lin Tian, Xiaodong Chen, Xiong Mei, and Yongli Nie interpreted the data. Qiao Yang, Lin Tian, and Jun Chen prepared the manuscript for publication and reviewed the draft of the manuscript. All authors have read and approved the manuscript.

References

- Cao JY, Dixon SJ (2016) Mechanisms of ferroptosis. *Cell Mol Life Sci* 73:2195–2209. <https://doi.org/10.1007/s00018-016-2194-1>
- Chen Y, Zhou Y, Ren R et al. (2024) Harnessing lipid metabolism modulation for improved immunotherapy outcomes in lung adenocarcinoma. *J ImmunoTher Cancer* 12:e008811. <https://doi.org/10.1136/jitc-2024-008811>
- Cui Y, Zhang Y, Zhao X et al. (2021) ACSL4 exacerbates ischemic stroke by promoting ferroptosis-induced brain injury and neuroinflammation. *Brain Behav Immun* 93:312–321. <https://doi.org/10.1016/j.bbi.2021.01.003>
- Denisenko TV, Budkevich IN, Zhivotovsky B (2018) Cell death-based treatment of lung adenocarcinoma. *Cell Death Dis* 9:117. <https://doi.org/10.1038/s41419-017-0063-y>
- Feng Q, Yang Y, Qiao Y et al. (2023) Quercetin ameliorates diabetic kidney injury by inhibiting ferroptosis via activating Nrf2/HO-1 signaling pathway. *Am J Chin Med* 51:997–1018. <https://doi.org/10.1142/S0192415X23500465>
- Lei G, Zhuang L, Gan B (2022) Targeting ferroptosis as a vulnerability in cancer. *Nat Rev Cancer* 22:381–396. <https://doi.org/10.1038/s41568-022-00459-0>
- Li Y, Li N, Xi L et al. (2024) Predictive value of the BDH2-MN2 nomogram model for prognosis at 3 months after receiving intravenous thrombolysis in patients with acute ischemic stroke. *Arch Med Sci* 20:1143–1152. <https://doi.org/10.5114/aoms/176740>
- Liu JZ, Hu YL, Feng Y et al. (2020) BDH2 triggers ROS-induced cell death and autophagy by promoting Nrf2 ubiquitination in gastric cancer. *J Exp Clin Cancer Res* 39:123. <https://doi.org/10.1186/s13046-020-01620-z>
- Lovly CM (2022) Expanding horizons for treatment of early-stage lung cancer. *N Engl J Med* 386:2050–2051. <https://doi.org/10.1056/NEJMe2203330>
- Rizzollo F, Escamilla-Ayala A, Fattorelli N et al. (2025) Agostinisin, BDH2-driven lysosome-to-mitochondria iron transfer shapes ferroptosis vulnerability of the melanoma cell states. *Nat Metab* 7:1851–1870. <https://doi.org/10.1038/s42255-025-01352-4>
- Scindia Y, Mehrad B, Morel L (2022) Labile iron accumulation augments T follicular helper cell differentiation. *J Clin Invest* 132:e159472. <https://doi.org/10.1172/JCI159472>
- Seah C, Karabacak M, Margetis K (2025) Transcriptomic imputation identifies tissue-specific genes associated with cervical myelopathy. *Spine J* 25:588–596. <https://doi.org/10.1016/j.spinee.2024.10.014>
- Tandon R, Levey AI, Lah JJ (2023) Machine learning selection of most predictive brain proteins suggests role of sugar metabolism in Alzheimer's disease. *J Alzheimers Dis* 92:411–424. <https://doi.org/10.3233/JAD-22068>
- Wei X, Li X, Hu S et al. (2023) Regulation of ferroptosis in lung adenocarcinoma. *Int J Mol Sci* 24:14614. <https://doi.org/10.3390/ijms241914614>
- Wei Z, Yu H, Zhao H et al. (2024) Broadening horizons: Ferroptosis as a new target for traumatic brain injury. *Burns Trauma* 12:tkad051. <https://doi.org/10.1093/burnst/ktad051>
- Wenqiao, Zang, Tao, Wang, Yuanyuan, Wang et al. Knockdown of long non-coding RNA TP73-AS1 inhibits cell proliferation and induces apoptosis in esophageal squamous cell carcinoma. *Oncotarget*, 2016, 7:19960-74.
- Wu J, Li H, Hu F et al. (2022) Stevioside attenuates osteoarthritis via regulating Nrf2/HO-1/NF-kappaB pathway. *J Orthop Translat* 38:190–202. <https://doi.org/10.1016/j.jot.2022.05.005>
- Wu XT, Wang YH, Cai XY et al. (2021) RNF115 promotes lung adenocarcinoma through Wnt/beta-catenin pathway activation by mediating APC ubiquitination. *Cancer Metab* 9:7. <https://doi.org/10.1186/s40170-021-00243-y>
- Xu Y, Zhang K, Ye Z et al. (2025) Nanomedicine initiates ferroptosis for enhanced lung cancer therapy. *Drug Deliv* 32:2527752. <https://doi.org/10.1080/10717544.2025.2527752>
- Yi, Luan, Yang, Yang, Ying, Luan et al. Targeting ferroptosis and ferritinophagy: new targets for cardiovascular diseases. *J Zhejiang Univ Sci B*, 2024, 25:1-22.
- Zhu W, Zhang Y, Yang L et al. (2025) Construction of a lung adenocarcinoma prognostic model based on KEAP1/NRF2/HO-1 mutation-mediated upregulated genes and bioinformatic analysis. *Oncol Lett* 29:155. <https://doi.org/10.3892/ol.2025.14902>
- Zuo L, Zou X, Ge J et al. (2025) The Nrf2-HMOX1 pathway as a therapeutic target for reversing cisplatin resistance in non-small cell lung cancer via inhibiting ferroptosis. *Cell Death Discov* 11:287. <https://doi.org/10.1038/s41420-025-02564-z>